Available online at www.sciencedirect.com
SCIENCE DIRECT®
Catalysis Today 87 (2003) 69–75
CATALYSIS TODAY
www.elsevier.com/locate/cattod

Photoresponse and AC impedance characterization of TiO_2–SiO_2 mixed oxide for photocatalytic water decomposition

The-Vinh Nguyen, O-Bong Yang*

School of Environmental and Chemical Engineering, Center for Advanced Radiation Technology, Chonbuk National University, 664-14, 1st Street, Dukjin-Dong, Chonju, Chonbuk 561-756, South Korea

Abstract

TiO_2–SiO_2 mixed oxides were prepared by sol–gel processes with one-stage (mix up fully hydrolyzed titania- and silica-sol), two-stage (with pre-hydrolysis) and modified two-stage synthesis routes. The photoresponse and AC impedance characterization of the derived catalysts are studied and correlated for the first time with the photocatalytic activities in water decomposition under UV illumination. Synergistic effects in terms of photocatalytic activity and electronic properties including band-gap energy, flat band potential and doping density were observed on atomically mixing TiO_2 and SiO_2 by the two-stage synthesis route. Meanwhile, the decline of photocurrent density were found on TiO_2–SiO_2 relative to bare TiO_2, which could be attributed to low quality crystalline structure of the former compared to that of the latter. The superior photocatalytic performance of TiO_2–SiO_2 is ascribed to the higher flat band potential, band-gap energy, and doping density than those of bare TiO_2.

Keywords: TiO_2–SiO_2 mixed oxide; Photoresponse; AC impedance; Photocatalytic water decomposition

1. Introduction

Since the discovery of Fujishima and Honda [1] with water splitting over TiO_2 electrodes in 1972, TiO_2 mediated heterogeneous photocatalysis has attracted greater attention because of its potential application to decomposition of water and hence vast of photocatalysts for this reaction including not only TiO_2-based but also non-TiO_2-based catalysts have been extensively studied for searching a renewable and inexpensive source of clean energy.

At present, TiO_2 is being much investigated for water decomposition reaction [2], degradation of organic pollutants [3] and dye-sensitized solar cells [4]. In order to enhance the photocatalytic activity, TiO_2 has been physicochemically combined with SiO_2 to take the advantage of resulting synergy effects including quantum-size and support effects [5]. Although the knowledge of the band edge position and photoresponse data are useful in photocatalysis, the synergistic effect in terms of such electronic properties on mixing TiO_2 and SiO_2 at atomic scale have not been much reported so far. The main purpose of this work is to synthesize various TiO_2–SiO_2 mixed oxides by sol–gel processes with different preparation procedures and then to characterize its electronic properties such as photocurrent density, band-gap energy, flat band potential and doping density. The photocatalytic performances of the derived catalysts are tested by water decomposition reactions under UV illumination.

* Corresponding author. Tel.: +82-63-270-2313; fax: +82-63-270-2306.
E-mail address: obyang@moak.chonbuk.ac.kr (O.-B. Yang).

0920-5861/$ – see front matter © 2003 Elsevier B.V. All rights reserved.
doi:10.1016/j.cattod.2003.10.014

2. Experimental

2.1. Preparation of gel-derived titania–silica mixed oxides

Fig. 1 shows the schematic diagram for the preparation of sample 1 (S1), sample 2 (S2), sample 3 (S3) and sample 4 (S4). S1 is prepared by one-stage synthesis route; S2 by two-stage synthesis route; S3 and S4 by modified two-stage route. Quantities and chemical composition of various kinds of samples are listed in Table 1.

2.1.1. Preparation of S1

S1 is prepared by slow mixing of titania-sol and silica-sol prepared separately under vigorous stirring at 80 °C for 2 h. The titania-sol is synthesized by mixing of two solutions at room temperature for 1 h: the first solution is a mixture of solvents (*i*-propanol and ethanol with volume ratio = 1:1) and diluted water; the second one is titanium(IV) isopropoxide (TTIP) (Junsei Chemical) with molar ratio of H_2O/TTIP = 20. The silica-sol is prepared as follows: a solution including the solvents and diluted water is mixed and refluxed with a tetraethyl orthosilicate solution

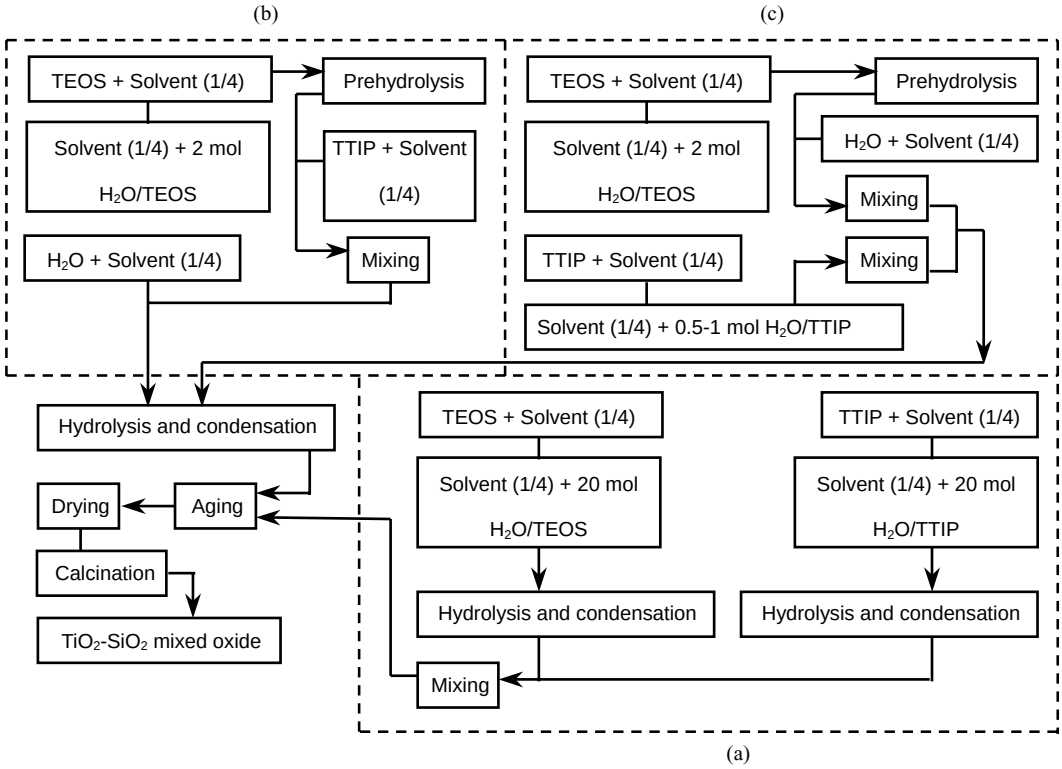

Fig. 1. Schematic diagram of preparation procedures of: (a) sample 1, (b) sample 2, and (c) samples 3 and 4.

Table 1
Quantities and chemical composition of various kinds of samples

Method	Material	TiO_2/SiO_2 (wt.%)	TTIP (mol)	TEOS (mol)	V_{R-OH} (EtOH–IPA) (ml)	35% HCl (mol)	H_2O (mol)
S1	TiO_2–SiO_2	50	0.263	0.35	160–160	0	12.26
S2	TiO_2–SiO_2	50	0.263	0.35	160–160	0.19	2.452
S3	TiO_2–SiO_2	50	0.263	0.35	160–160	0.056	2.452
S4	TiO_2–SiO_2	50	0.263	0.35	160–160	0.056	2.452

(TEOS) (Aldrich Chemical), and pre-hydrolyzed at 80 °C for 2 h with vigorous stirring (ca. 1000 rpm) (with the molar ratio of $H_2O/TEOS = 20$).

The obtained sol–gel is aged at room temperature for 24 h and then removed the solvent in a vacuum evaporation system at 50 °C. Thereafter, the gel is dried in an oven at 70 °C for 24 h. The resulting xerogel is calcined in static air at desired temperatures for 2 h.

2.1.2. Preparation of S2

S2 is prepared by slow mixing of pre-hydrolyzed TEOS solution and TTIP solution under vigorous stirring (ca. 1500 rpm) at 80 °C for 1 h. The pre-hydrolyzed TEOS solution is prepared by mixing and refluxing of two solutions at 80 °C for 2 h: the first solution consists of solvents and diluted water with pH 1 controlled by 35% hydrochloric solution; the second one is a mixture of TEOS solution (with the molar ratio of $H_2O/TEOS = 2$) and solvents. The prepared mixture is fully hydrolyzed with solvents and diluted water of pH 1 under refluxing at 80 °C for 2 h. The other procedures are similar to that of S1 as shown in Fig. 1. In this preparation, the molar ratio of $H_2O_{(total)}/(TEOS + TTIP)$ or R_w is 4.

2.1.3. Preparation of S3

S3 is prepared by the similar method of S2 except that the time for TEOS pre-hydrolysis is 1 h, the molar ratio of $H_2O/TTIP = 0.5$ in the pre-hydrolysis process of TTIP and the sequence of water introduction into the hydrolysis process is slightly different from preparation procedures of S2 as shown in Fig. 1.

2.1.4. Preparation of S4

The preparation procedures of S3 are repeated except for the molecular ratio of $H_2O/TTIP = 1$. For comparison, TiO_2 (P-25, Degussa) and SiO_2 (amorphous, Strem) are employed as-received.

2.2. Photocatalytic water decomposition

Photocatalytic reaction is carried out in a batch reactor with a quartz inner irradiation type cell. A suspension of catalyst (1.5 g) and diluted water (700 ml) is degassed completely by bubbling nitrogen gas until oxygen free and then nitrogen is filled up the reactor at atmospheric pressure. The catalyst is suspended by stirring and irradiated by a high-pressure Hg lamp (450 W). The evolution gases are analyzed by GC equipped with TCD and molecular sieve 5 A capillary column (30 m).

2.3. Characterization

Photocatalysts are characterized by using nitrogen adsorption for BET specific surface area at 77 K (Micromeritics ASAP 2100), X-ray powder diffraction (XRD, Cu Kα radiation, Rigaku), UV-Vis diffuse reflectance spectroscopy (UV-Vis DRS, Shimadzu-UV 525), photocurrent density–potential measurement and capacitance–voltage (*C–V*) technique. The photocurrent of each TiO_2, SiO_2, and TiO_2–SiO_2 electrode is measured by using a scanning potentiostat (EG&G 273) with software (EG&G M542) and a high-pressure Hg lamp (450 W) as the irradiation source. The setup of *C–V* measurement is consisted of a lock-in amplifier (EG&G 5210) coupled with a potentiostat (EG&G 273) and software (EG&G M398). The working electrodes used for photocurrent and *C–V* measurement are prepared by coating method: photocatalysts are ground in mortar and pestle before mixing and sonicating with diluted water (10 min) to obtain coating suspensions (0.8 M); after coating and drying (in static air at room temperature) on a disk glassy carbon electrode (MF-2012, BAS) with the surface area and also the area exposed to light of 7.065×10^{-6} m^2, a solution of Nafion (5%, containing 15–20% water, Aldrich) as a binder is covered over the layer of photocatalyst. The derived electrodes are dried in an oven at 100 °C for 30 min. The characterization of electrodes is carried out in an electrochemical cell with 0.1 M Na_2SO_3 electrolyte at pH 9, using anodes of photocatalysts as the working electrodes, a Pt wire as the counter electrode and a Ag/AgCl/3 M NaCl electrode as the reference electrode. The data of *C–V* are used for evaluating the flat band potential and dopant density by means of Mott–Schottky equation:

$$C^{-2} = \frac{2(V - V_{fb} - KT/e)}{\varepsilon\varepsilon_0 e N_d} \quad (1)$$

where C is the total measured capacitance, ε the dielectric constant of the material, ε_0 the permittivity of the vacuum, e the electron charge, N_d the concentration of donors in n-type semiconductor.

3. Results and discussion

3.1. Characterization of the photocatalysts

Fig. 2 shows the XRD patterns of the catalysts in which the rutile phase of S1 appears at lower temperature compared to that of S2. Gel-derived TiO_2–SiO_2 mixed oxides prepared by two-stage synthesis routes exhibit the diffraction peaks corresponding to anatase phase only. Even though increasing the degree of crystallinity with increasing calcination temperature, there is no phase transformation from anatase to rutile up to 900 °C. This result suggests that two-stage synthesis route leads to the formation of the atomically well mixed structure between TiO_2 and SiO_2, which retards the phase transformation to the rutile and the polycrystalline due to the strong bonding of Ti–O–Si linkage. On the other hand, the rutile peak obviously appears at 750 °C and fully developed at 900 °C with significant characteristics of polycrystalline in gel-derived TiO_2–SiO_2 mixed oxides synthesized by one-stage synthesis routes (S1). However, the absolute crystallinities of TiO_2–SiO_2 mixed oxides are much less than that of TiO_2 (P-25) which is probably attributable to the interference of SiO_2 as an amorphous phase into TiO_2 lattice.

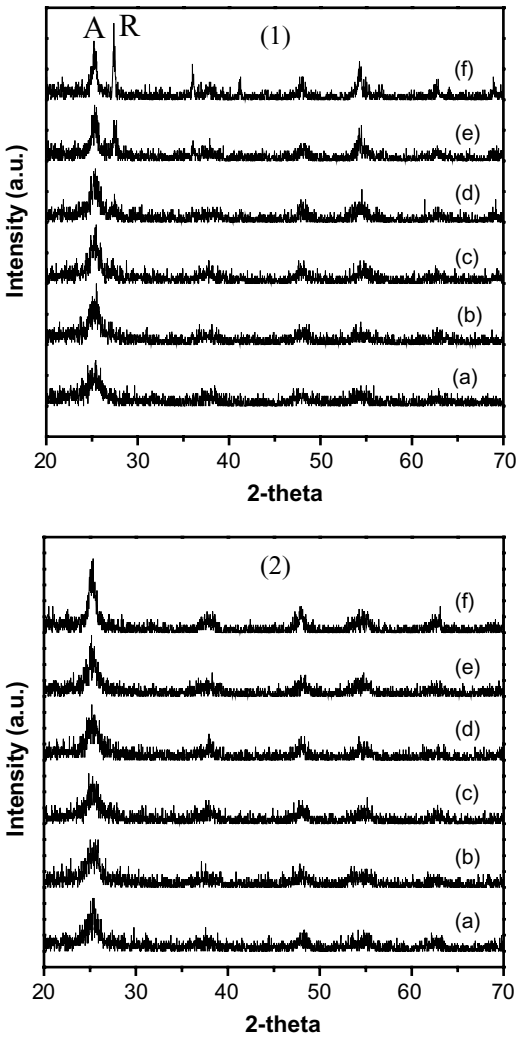

Fig. 2. X-ray diffraction patterns of S1 and S2 at different calcination temperatures: (1) S1, (2) S2; (a) 300 °C, (b) 400 °C, (c) 500 °C, (d) 600 °C, (e) 750 °C, and (f) 900 °C; A: anatase, R: rutile.

The BET specific surface areas of SiO_2 and TiO_2–SiO_2 (S2) are substantially higher than that of TiO_2 (P-25) as shown in Table 2. However, the BET specific surface areas of TiO_2–SiO_2 mixed oxides significantly depend on the preparation procedures: S1 > S2 > S3 ≫ S4. The result could be attributable to the effect of molar ratio of water to TTIP as well as the mixing sequence of metal alkoxides and hydrolysant. On the other hand, the pore volume considerably decreases from S1 to S4: S1 (0.35 cm^3/g) > S2 (0.07) > S3 (0.05) ≫ S4 (0.01), which is consistent with a previous study [6] in which pre-hydrolysis was generally found to lead to lower porosity. Consequently, BET specific surface area also decreases dramatically from S1 to S4.

The band-gap energies calculated by using UV-Vis DRS spectra with the equation, E (eV) $\cong$ $1239.95/\lambda$ (nm), are shown in Table 2. It is apparent that the band-gap energies of TiO_2–SiO_2 mixed oxides are higher than that of bare TiO_2 (P-25), which are ascribed to the quantum-size and support effect on mixing TiO_2 and SiO_2 at atomic scale [5].

Photocurrent density is defined as the difference between light and dark current density. The photocurrent densities of TiO_2, SiO_2, and TiO_2–SiO_2 with the applied potentials vs. Ag/AgCl are shown in Fig. 3. The photocurrent densities as high as 14.0 $\mu A/cm^2$ at −0.8 V and 31 $\mu A/cm^2$ at +0.5 V vs. Ag/AgCl are measured on TiO_2. Whereas, those of SiO_2 and TiO_2–SiO_2 mixed oxides are almost equal to zero between −0.8 and +0.5 V vs. Ag/AgCl, the potential range in which the TiO_2, SiO_2, and TiO_2–SiO_2 are

Table 2
S_{BET}, electronic properties, and hydrogen evolution over various photocatalysts

Photocatalyst	S_{BET} (m^2/g)	E_g (eV)	E_{fb} (V)	N_d (m^{-3})	Hydrogen evolution (μmol for 24 h)
TiO_2	50	3.00	−0.654	6.46×10^{25}	Trace
SiO_2	292	8–8.9 [10]	–	–	Trace
S1-750	331	3.06	−0.692	1.12×10^{26}	12.2
S2-750	220	3.20	−1.045	1.34×10^{27}	25.5
S3-750	169	3.18	−1.108	3.34×10^{26}	15.8
S4-750	41	3.18	−0.732	2.93×10^{26}	14.2

insulating in dark. The results suggest that the presence of silica in the TiO_2–SiO_2 mixed oxide substantially increases the recombination of photo-excited electrons and holes. The photocurrent densities are decreased to nearly zero as increasing the SiO_2 content in TiO_2–SiO_2 (Fig. 4), which indicates the role of SiO_2 to suppress the photocurrent of resulting catalysts. For this reason, the photocurrent density of SiO_2 and TiO_2–SiO_2 mentioned in the text refer to the photocurrent density beyond overpotential. As scanning passes beyond overpotential, the photocurrent density of TiO_2 is still much higher than those of SiO_2 and TiO_2–SiO_2, which might be attributed to the high crystallinity of TiO_2 in comparison with SiO_2 and TiO_2–SiO_2 as observed in the XRD patterns in Fig. 2. The highest photocurrent density is observed on S1 with the highest crystallinity among the catalysts as shown in Fig. 5, which is consistent with the case of bare TiO_2. Because of the wavelike nature of

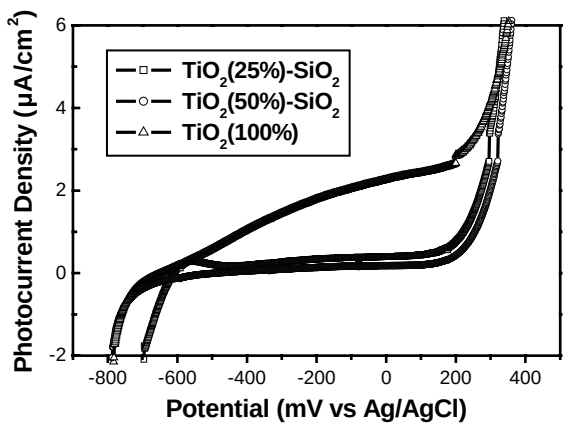

Fig. 4. The photocurrent density of TiO_2–SiO_2 with different composition of TiO_2.

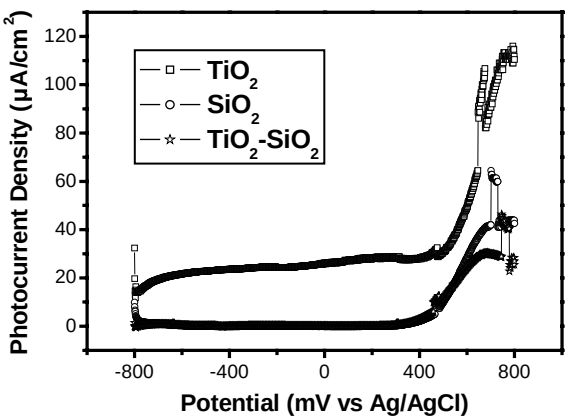

Fig. 3. The photocurrent density of TiO_2, SiO_2, and TiO_2–SiO_2 (S2-750).

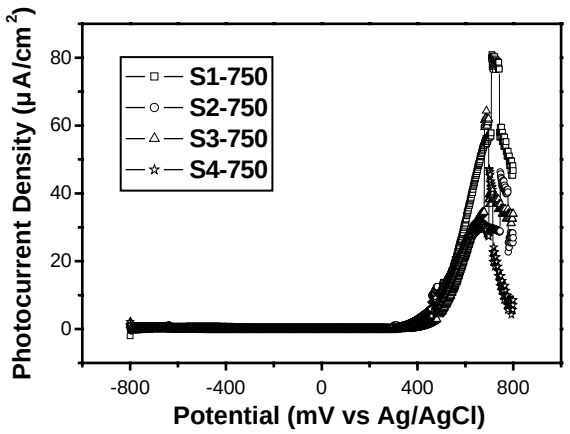

Fig. 5. The photocurrent density of S1–S4 at calcination temperature of 750 °C.

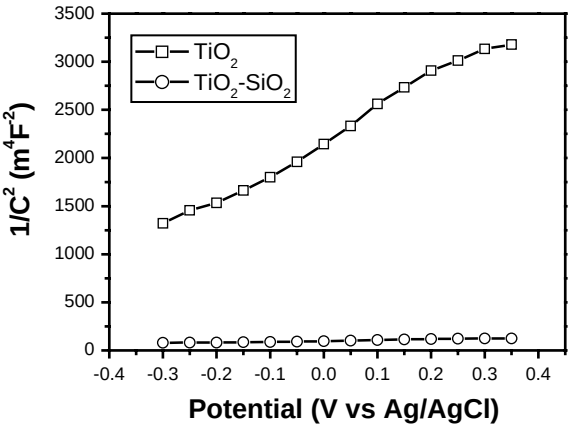

Fig. 6. M–S plot of TiO_2 and TiO_2–SiO_2 (S2-750) at AC frequencies of 1 kHz.

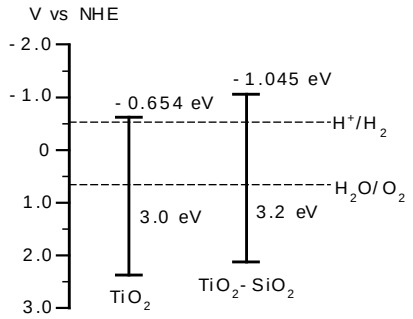

Fig. 7. Band edge of TiO_2 and TiO_2–SiO_2 (S2) are compared with the redox potential for hydrogen and oxygen evolution at pH 9.

photo-excited electrons, they can move through crystalline structure most effectively when that structure is nearly perfect. Irregularity due to the low crystallinity of TiO_2–SiO_2 compared to bare TiO_2 diminishes electron mobility resulting the substantial increase of the recombination of photo-excited electron–hole pairs.

It is well known that the flat band potential (V_{fb}) of a semiconductor can be obtained from the intercept of the Mott–Schottky plot [7] by using Eq. (1). In this work, the flat band potentials are measured at 1 kHz AC frequency that is typically used for the measurement of Mott–Schottky plot [8]. Fig. 6 depicts the Mott–Schottky plots of TiO_2 and TiO_2–SiO_2 at 1 kHz AC frequency. It is found that the flat band potential of TiO_2–SiO_2 (S2) with −1.045 eV vs. NHE is significantly higher than that of TiO_2 with −0.654 eV vs. NHE. The flat band potential of S1–S4 are also determined as shown in Table 2: S3 ≅ S2 > S4 > S1. From the data of band-gap energies along with the flat band potentials of the photocatalysts, the schematic diagram of band energy levels of TiO_2 and TiO_2–SiO_2 (S2) is presented in Fig. 7.

Doping density (N_d) can be obtained from the slope of the Mott–Schottky plots by means of Eq. (1). Table 2 shows the doping densities of TiO_2 and TiO_2–SiO_2 prepared by different methods at 1 kHz AC frequency: S2 ($1.34 \times 10^{27}\,m^{-3}$) ≫ S3 ($3.34 \times 10^{26}\,m^{-3}$) > S4 ($2.93 \times 10^{26}\,m^{-3}$) > S1 ($1.12 \times 10^{26}\,m^{-3}$) ≫ TiO_2 ($6.46 \times 10^{25}\,m^{-3}$), indicating that S1 shows the lowest doping density among TiO_2–SiO_2 catalysts. It is found that the order of doping density is reciprocally proportional to those of photocurrent and crystallinity. Accordingly, the lowest doping density of S1 is consistent with its high photocurrent density as shown in Fig. 5. Akikusa and Khan [9] reported that the "metallization" of semiconductor due to excess doping density made to a low photocurrent density.

In summary, the photoresponse and AC impedance characterization of TiO_2, SiO_2, and TiO_2–SiO_2 indicate that atomically mixed TiO_2–SiO_2 (S2) shows superior properties such as flat band potential and doping density compared to those of TiO_2 alone. However, photocurrent density of TiO_2–SiO_2 is much lower than that of bare TiO_2 due to low quality crystalline structure of TiO_2–SiO_2. Synergistic effects on atomically mixing TiO_2 and SiO_2, i.e. quantum-size and support effects have been reported in a previous review of Gao and Wachs [5].

3.2. Photocatalytic water decomposition

Table 2 shows the rate of hydrogen formation over various kinds of photocatalysts: S2 (25.5 μmol for 24 h) > S3 (15.8 μmol for 24 h) > S4 (14.2 μmol for 24 h) > S1 (12.2 μmol for 24 h). Trace amount of hydrogen is evolved over TiO_2 and SiO_2 that is in agreement with a previous report [2]. Meanwhile, the highest hydrogen evolution rate as high as 25.5 μmol for 24 h is observed on TiO_2–SiO_2 (S2) mixed oxide. As shown in Fig. 3, the highest photocurrent density is found over TiO_2, which strongly suggests that the photocatalytic activity could not directly corre-

late with photocurrent density. However, TiO_2–SiO_2 mixed oxide (S2) shows the flat band potential as high as −1.045 V vs. NHE, which is much higher than that of bare TiO_2 with −0.654 V vs. NHE (Fig. 7). Also, the doping density of TiO_2–SiO_2 mixed oxide is higher than that of bare TiO_2 as shown in Table 2. Accordingly, it is concluded that the superior performance of S2 in photocatalytic water decomposition to hydrogen might be attributed to not only high flat band potential but also high doping density. The higher flat band potential, the stronger reduction power and therefore, the more superior photoproduction to hydrogen of TiO_2–SiO_2 (S2) compared to bare TiO_2. In addition, it is worth noting that the superior performance of S2 is also in agreement with the high band-gap energy and specific surface area, which indicates that optimized textural and electronic properties are necessary to achieve excellent photocatalytic performance.

4. Conclusions

Synergistic effects in terms of photocatalytic activity and electronic properties including band-gap energy, flat band potential, and doping density are observed on atomically mixing TiO_2 and SiO_2 by two-stage (with pre-hydrolysis) synthesis routes. Meanwhile, the photocurrent density of TiO_2–SiO_2 mixed oxide is lower than that of bare TiO_2, which is probably due to the interference of SiO_2 as an amorphous phase into TiO_2 lattice rendering the crystallinity of TiO_2–SiO_2 declined. Conclusively, the superior photocatalytic performance of TiO_2–SiO_2 is ascribed to the higher flat band potential, band-gap energy, and doping density than those of TiO_2 alone in photocatalytic water decomposition to hydrogen production under UV irradiation.

References

[1] A. Fujishima, K. Honda, Nature 37 (1972) 238.
[2] T. Takata, A. Tanaka, M. Hara, J.N. Kondo, K. Domen, Catal. Today 44 (1998) 19.
[3] A. Fujishima, K. Hashimoto, T. Watanabe, TiO_2 Photocatalysis: Fundamentals and Applications, BKC, Tokyo, 1999.
[4] R.D. McConnell, Renewable Sustain. Energy Rev. 6 (2002) 273–295.
[5] X. Gao, I.E. Wachs, Catal. Today 51 (1999) 245.
[6] D.C.M. Dutoit, M. Schneider, A. Baiker, J. Catal. 153 (1995) 165.
[7] F. Mollers, H.J. Tolle, R. Memming, J. Electrochem. Soc. 121 (1974) 1160.
[8] B. O'Regan, M. Graetzel, Nature 353 (1991) 737.
[9] J. Akikusa, S.U.M. Khan, Int. J. Hydrogen Energy 22 (9) (1997) 878–881.
[10] G.A. Zacheis, K.A. Gray, P.V. Kamat, J. Phys. Chem. B 105 (2001) 4719.